OPEN ACCESS

Received: 21-05-2026

Accepted: 13-06-2026

المجلد15،العدد1، يونيو 2026
Volume 15, Issue1, June 2026
المجلة العلمية لكلية التربية
The Scientific Journal of the Faculty of Education

Unveiling the Optical Properties, Adsorption Capacity, and Efficient Reusability of Natural Nanoclay for Remediation of Anionic Direct Dye from Wastewater

Mohammed A.H. Dhaif-Allah[1*], Waled Abdo Ahmed[2*], Waleed ALGhaberi[2], Ahmed Qaid[3], Morad G.S Al-asbahi[4], Fares H. AL-Ostoot[5,6] *

[1]Department of Agricultural, Faculty of Agriculture, Thamar University, Dhamar, 00967, Yemen.

[2]Department of Chemistry, Faculty of Education, Thamar University, Dhamar, 00967, Yemen

[3]Department of Chemistry, Faculty of Applied Sciences, Thamar University, Dhamar, 00967, Yemen

[4]Department of Microbiology, Faculty of Applied Sciences, Thamar University, Dhamar, 00967, Yemen.

[5]Department of Biochemistry, Faculty of Education and Science, Albaydha University, Albaydha, 00967, Yemen.

[6]Department of Biological, Chemical, and Pharmaceutical Sciences and Technologies (STEBICEF), University of Palermo, Palermo, Italy.

Dr. Mohammed A.H. Dhaif-Allah, mdhaif2014@gmail.com, mdhaif2014@tu.edu.ye

Dr. Waled Abdo Ahmed, Waled.abdulrab@tu.edu.ye

Abstract

This investigation focused on the optical properties and performance natural nanoclay (Montmorillonite, MNC) as an adsorbent for the removal of Anionic Direct Red 80 dye from aqueous solutions. Pristine and post-adsorption materials were systematically evaluated using Scanning Electron Microscopy with Energy-Dispersive X-ray Spectroscopy (SEM-EDX) and Fourier-Transform Infrared (FTIR) analyses confirmed significant mutual interactions between the nanoclay framework and the dye molecules. Optical characterization revealed a sharp transmission edge at 288 nm and an ultra-wide bandgap of 3.8 eV, supporting the material's structural stability and suitability for the adsorption process. Batch adsorption experiments (pH 7.0, 25 °C) demonstrated outstanding performance, achieving 99.13% removal efficiency within 60 minutes with a maximum adsorption capacity (q_e) of 49.57 mg/g. The adsorption mechanism was governed by a synergistic combination of hydrogen bonding, $n \longrightarrow \pi$ interactions, and surface complexation. Furthermore, the nanoclay exhibited excellent reusability, maintaining removal efficiencies of 91.67% and 82.59% in the second and third cycles, respectively. These findings indicate that natural nanoclay is a scalable, cost-effective, and eco-friendly solution for the comprehensive treatment of synthetic dyes and industrial pollutants.

Keywords: adsorbent nanoclay, anionic direct dye, removal efficiency, adsorbent reusability

*

Cite this article as: Dhaif-Allah, M. A. H& Ahmed, W. A& ALGhaberi, W& Qaid, A& Al-asbah,M.& AL-Ostoot (2026). T *Unveiling the Optical Properties, Adsorption Capacity, and Efficient Reusability of Natural Nanoclay for Remediation of Anionic Direct Dye from Wastewater The Scientific Journal of The Faculty of Education, 15*(1), 769 -787.

المجلد15، العدد1، يونيو 2026
Volume 15, Issue1, June 2026
المجلة العلمية لكلية التربية
The Scientific Journal of the Faculty of Education

OPEN ACCESS

تاريخ الاستلام: 21/ 05/ 2026
تاريخ القبول: 13/ 06/ 2026

((تعيين الخواص الضوئية وقدرة الامتزاز، وكفاءة إعادة استخدام الطين النانوي الطبيعي لإزالة الصبغة المباشرة الأنيونية الملوثة للماء))

د. محمد علي حسين ضيف الله [*]
mdhaif2014@tu.edu.ye

أ.م. د. وليد عبده أحمد عبدالرب **
Waled.abdulrab@tu.edu.ye

وليد الغابري*** أحمد قائد****، مراد جميل سعيد الأصبحي*****، فارس حسن العستوت*****

ملخص :

ركزت هذه الدراسة على الخصائص الضوئية وأداء الطين النانوي الطبيعي (مونتموريلونيت) كمادة ماصة لإزالة الصبغة الأيونية المباشرة الحمراء من المحاليل المائية. تم تقييم المواد قبل الامتزاز وبعده بشكل منهجي، باستخدام المجهر الإلكتروني الماسح، مع مطيافية فحص مكونات الطين النانوي (SEM-EDX)، وأكدت تحليلات الأشعة تحت الحمراء (FTIR) وجود تفاعلات متبادلة بين هيكل الطين النانوي وجزيئات الصبغة. كشفت الخصائص الضوئية عن حافة نفاذية حادة عند 288 نانومتر وفجوة نطاق واسعة تبلغ 3.8 إلكترون فولت، ما يدعم استقرار بنية المادة وملاءمتها لعملية الامتزاز. أظهرت تجارب الامتزاز (بالأس الهيدروجيني 7.0، ودرجة حرارة 25 درجة مئوية) أداءً متميزًا، حيث حققت كفاءة إزالة بلغت 99.13% خلال 60 دقيقة مع سعة امتزاز قصوى (qe) تبلغ 49.57 ملغم/غرام. تخضع آلية الامتزاز لتأثير تآزري من الروابط الهيدروجينية، وتفاعلات $\pi \longrightarrow n$، وتكوين معقدات سطحية. علاوة على ذلك، أظهر الطين النانوي قابلية ممتازة لإعادة الاستخدام، حيث حافظ على كفاءة إزالة بلغت 91.67% و82.59% في الدورتين الثانية والثالثة على التوالي، وتشير هذه النتائج إلى أن الطين النانوي الطبيعي حلا قابل للتطوير، وفعال من حيث التكلفة، وصديق للبيئة، لمعالجة الأصباغ والملوثات الصناعية.

.الكلمات المفتاحية: النانوي المازّ، الصبغة المباشرة الأنيونية، كفاءة الإزالة، قابلية إعادة استخدام المادة المازّة

[*] علوم بيئية (تربة ومياه) – كلية الزراعة – جامعة ذمار
** كيمياء تحليلية – كلية التربية – جامعة ذمار
***قسم الكيمياء، كلية العلوم التطبيقية، جامعة ذمار، ذمار، اليمن .
****قسم الأحياء الدقيقة، كلية العلوم التطبيقية، جامعة ذمار، ذمار، اليمن .
*****قسم الكيمياء الحيوية، كلية التربية والعلوم، جامعة البيضاء، البيضاء، اليمن .
******قسم العلوم والتقنيات البيولوجية والكيميائية والصيدلانية(STEBICEF) ، جامعة باليرمو، باليرمو، إيطاليا.

للاقتباس: ضيف الله ، م. ع. ح؛ عبدالرب، و. ع. أ.؛ الغابري، و. قائد، أ؛ الأصبحي، م؛ العستوت، ف. (2026). (تعيين الخواص الضوئية وقدرة الامتزاز ، وكفاءة إعادة استخدام الطين النانوي الطبيعي لإزالة الصبغة المباشرة الأنيونية الملوثة للماء) ، *المجلة العلمية لكلية التربية*، *15* (1)، 976- 787

Introduction

Nanomaterials, defined by possessing at least one dimension in the range of 1–100 nm, have revolutionized materials science. At this reduced scale, materials exhibit unique physicochemical, optical, and mechanical properties due to high surface-area-to-volume ratios and quantum confinement effects (Zarei S., Sadeghi M., et.al 2018), (Murad Q.A. Al-Gunaid, et.al 2023), (Alkanad Khaled, et.al 2021), (Anupama, B. H, et.al 2021), (Gayitri H M, et.al 2020). Consequently, nanoparticles (NPs) have become fundamental building blocks in modern industries, ranging from targeted drug delivery, opto-electrical devices and solar cells to aerospace manufacturing (Mahdavinia G. R., et.al 2014), (Murad Q. A. AL-Gunaid, et.al 2023), (Gayitri H.M., et.al 2023), (Somesh T. E, et.al 2018). However, as the demand for advanced nanomaterials grows, there is a concurrent push toward finding greener, more sustainable, and cost-effective alternatives to synthetically engineered nanoparticles (Kumar R., Kumar M., et.al 2020), (Mohammed A. H. Dhaif Allah et.al 2018), (Murad Q. A. Al-Gunaid, et.al 2025). Among the diverse classes of NPs available today, natural nanoclays (Montmorillonite, MNC) have emerged as highly promising, eco-friendly candidates (Almasri D. A., et.al 2018), (Mohammed A. H. Dhaif Allah et.al 2018). Nanoclays refer to layered mineral silicates typically 1 nm thick and several hundred nanometers in length that are derived from natural clay deposits (Zaharia C., et.al 2012). The most widely studied type is montmorillonite (MNC), a 2:1 smectite clay composed of an octahedral alumina sheet sandwiched between two tetrahedral silica sheets (Mittal A., et.al 2009). This layered structure grants natural nanoclay exceptional features, including a massive cation exchange capacity, high aspect ratios, high thermal stability, and excellent mechanical strength (Sonawane S. H., et.al 2009). Due to these diverse properties, MNC finds widespread applications as a mechanical reinforce in polymer nanocomposites (Mahvi A. H., et.al 2020), a high-performance cement additive, and a reliable carrier for controlled drug release. Despite rapid global industrialization, severe environmental degradation remains a critical byproduct. The contamination of freshwater channels by untreated industrial effluents has reached an alarming rate, with the textile industry alone accounting for nearly 20% of global industrial water pollution (Mouton J., et.al 2022). Among the various pollutants present in wastewater, synthetic dyes present the stubbornest challenge (Zahoor I., et.al 2024), (Shashikala B.S, et.al 2021). Dyes are chemically stable, resistant to biological degradation, and impervious to light and oxidation (Al-Ali A., et.al 2024). Anionic direct dyes, such as Anionic Direct Red 80 dye, in particular, are highly water-soluble and carry negative charges, making them exceptionally difficult to separate (Mittal V., 2010). When discharged into aquatic bodies, they block sunlight penetration, inhibit photosynthesis, and pose severe carcinogenic and mutagenic threats to human health (Abd El-Latif M. M., et.al 2010). To solve these pressing wastewater problems, conventional techniques like chemical precipitation, membrane filtration, and advanced oxidation have been deployed. However, these methods often suffer from high operational costs and the generation of secondary toxic sludge (Salam M. A., et.al 2017). Adsorption stands out as the most attractive alternative due to its simplicity, efficiency, and

low cost. This is precisely where natural nanoclay proves its immense importance (Sadeghi M., et.al 2024). Because nanoclays are abundant and inherently non-toxic, they offer an economically viable and biocompatible alternative to synthetic adsorbents (Hassaan M. A., et.al 2017). While the potential of nanoclay as an adsorbent is well recognized, optimizing its performance specifically for anionic direct dyes requires deeper investigation into its optical behaviors and continuous recyclability. To address this need, this study aims to investigate the optical properties and adsorption performance of montmorillonite as a natural nanoclay adsorbent for removing anionic direct dye from wastewater. Furthermore, it characterizes the mutual interactions between the adsorbent nanoclay and the target dye using detailed Scanning Electron Microscopy with Energy-Dispersive X-ray Spectroscopy (SEM-EDX) and Fourier-Transform Infrared (FTIR) analyses, while evaluating the optical transmittance and absorption edges of the pure nanoclay to determine its suitability and efficiency for the adsorption process. Ultimately, this work assesses the reusability and efficiency of nanoclay across consecutive cycles to prove its viability as a scalable, cost-effective, and long-term solution for industrial wastewater treatment.

Experimental Section

Materials and Reagents

The natural nanoclay (Montmorillonite, MNC) was purchased from Sigma Aldrich (India). Prior to use, the nanoclay was dried in an oven at 60–70 °C for 2 hours to remove any residual moisture, after which the dried powder was utilized directly in the batch adsorption experiments. (According to the manufacturer's technical specifications product No. 281522, the nanoclay has specific surface area (BET) of ranging from 220 to 270 mg^2/g and the total pore volume is typically ranges from 0.30 to 0.40 cm^3/g, with an average pore diameter of approximately between 4.0 nm and 6.3 nm). The Anionic Direct Red 80 dye, (purity > 98%) was also supplied by Sigma-Aldrich (India) and was used as received without further purification or processing. The chemical structure of the anionic direct red dye is illustrated in Fig. 1. Distilled water was used throughout the study for the preparation of all aqueous dye solutions and for washing procedures. To maintain neutral conditions, the initial adsorption process was conducted at a fixed pH of 7.0.

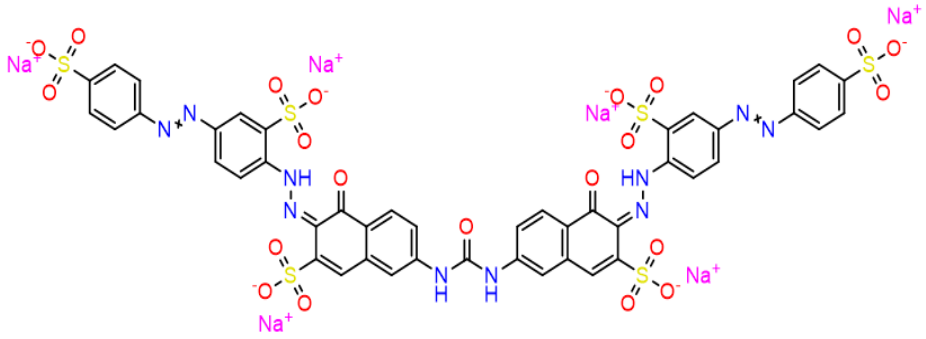

Fig.1. Chemical structure of pure anionic direct red dye.

Batch Adsorption-Desorption Experiments

The working dye solutions (50 mg/L) were prepared by appropriate dilution of concentrated stocks; the stock of anionic Direct Red dye was prepared by dissolving 0.05 g of powder in 100 mL of distilled water. For each adsorption run, 50 mL of the respective dye solution was transferred into a conical flask, and the initial pH 7.0 was fixed and precisely adjusted using 0.1 M HCl or 0.1 M NaOH, following the procedure reported elsewhere in the literature (Mohammed A. H. Dhaif Allah, et.al 2025), (Ait Akbour R., et.al 2018). Then, a fixed dosage of 0.05g of adsorbent nanoclay (equivalent to 1 g/L) was introduced into the flasks, and the suspensions were agitated at moderate speed on a magnetic stirrer. Following the equilibration period, the adsorbent was separated from the liquid phase via centrifugation 5000 rpm for 10 min. The residual concentration of Direct Red dye was quantified using a UV-Vis spectrophotometer by measuring absorbance at the maximum wavelength (λ_{max}) of 628 nm (scanned within a 200–800 nm range). The adsorption capacity (q_e, mg/g) and the Removal efficiency (%) were calculated using the following equations (1) and (2):

$$Adsorption\ Capacity\ (q_e) = \frac{(C_0 - C_e) \times V}{W} \qquad (1)$$

$$Removal\ Efficiency\ (\%) = \frac{A_0 - A_C}{A_0} \times 100 \qquad (2)$$

Where, C_e is equilibrium concentration (mg/L), V is the volume in Liters and W is adsorbent weight in (grams), A_0 is the initial absorbance (of pure dye) and Ac is equilibrium absorbance (during adsorption with nanoclay at certain time). After finished the adsorption process for removal the dye from solution, the desorption of nanoclay was adjusted by collect the nanoclay and transfer it to beaker contain 20 ml NaOH and stir for 30 min to remove the remain direct dye that stuck on the surface of nanoclay. After that, the washing of nanoclay several time by distilled water until the neutralized and then centrifuged it to remove water. Finally, the collect nanoclay was dried at 60 °C in oven for 2 hrs, then it can have recycled to removal of fresh direct dye again.

Characterization Techniques

To investigate the physicochemical and structural properties of the material, various characterization techniques were deployed. The vibrational modes and functional groups of the samples were characterized by Fourier transform infrared (FTIR) spectroscopy in the wavenumber range of 4000–400 cm^{-1}, sing a JASCO 4100 spectrometer (Japan). The morphological behavior and surface microstructures of the samples were recorded using a Zeiss-108A scanning electron microscope (SEM) (Germany). The elemental composition of the sample was simultaneously determined and confirmed by energy-dispersive X-ray analysis (EDAX). Finally, the optical properties and transmittance parameters were analyzed via UV-Visible spectroscopic studies, established on a JENWAY-6705 spectrophotometer (UK) in the wavelength range of 200–800 nm.

Results and Discussion

Structural Analysis

The elemental composition of the natural nanoclay was determined using EDAX, and the results are depicted in Fig.2a (with elemental percentages provided in the inset table).

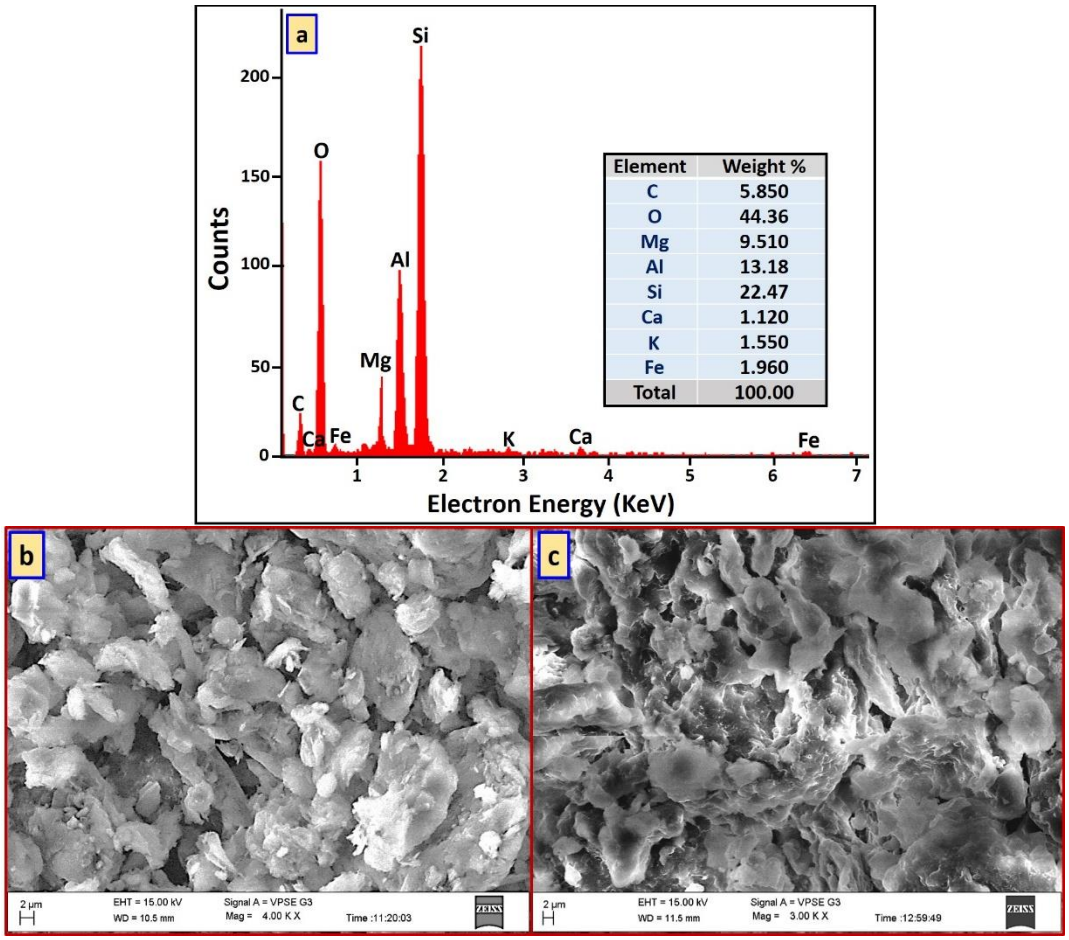

Fig.2. a) EDAX of natural nanoclay, SEM images of natural nanoclay b) before, and c) After anionic direct dye adsorption.

The pristine material is primarily composed of Oxygen (44.36 wt%) silicon (22.47 wt%), aluminum (13.18 wt%), and Magnesium (9.510 wt%), which is consistent with the typical aluminosilicate framework of natural smectite or montmorillonite clay minerals. Trace amounts of Calcium (1.120 wt%), Potassium (1.550 wt%), and Iron (1.960 wt%) were also detected, representing the exchangeable interlayer cations and native structural elements within the pristine clay matrix. Additionally, the analysis recorded a Carbon content of 5.850 wt% (11.73 Atom%). This minor carbon concentration is attributed to background signals from the conductive carbon adhesive tape utilized to secure the powder sample onto the SEM stub during analysis,

alongside trace organic matter naturally embedded within the clay deposit. The total elemental distribution sums logically to 100%, establishing a clear, transparent baseline profile for the natural adsorbent prior to its application in the batch dye removal process.

Figure 2b, c illustrates the SEM morphological structure of natural nanoclay before and after anionic direct dye adsorbed. From Fig. 2b, the natural nanoclay texture resembles irregularly shaped, aggregated flakes of varying sizes with a specific surface area, as reported elsewhere (Farhad M., et.al 2017), (Ukkund S.J., et.al 2021). As a result of that, the natural nanoclay possess a high efficiency of adsorption for many pollutants and dyes (Murray H. H., 1991). Figure 2c presents the SEM micrographs of the natural nanoclay after adsorption of anionic direct dye. The SEM images reveal noticeable morphological changes compared to the pristine adsorbent. Specifically, variations in contrast and shading distributed across the surface and within the accessible interlayer spaces indicate topographical changes and surface roughness alterations. These visual developments provide evidence of pore coverage and surface loading by the dye molecules. This observation confirms the successful interaction between the adsorbate and adsorbent phases.

Figure 3 presents the Fourier-transform infrared (FTIR) spectra for the pure anionic direct dye, pristine natural nanoclay, and the resultant the natural nanoclay after adsorption of anionic direct dye, analyzed across the wavenumber range of 4000–500 cm^{-1}.

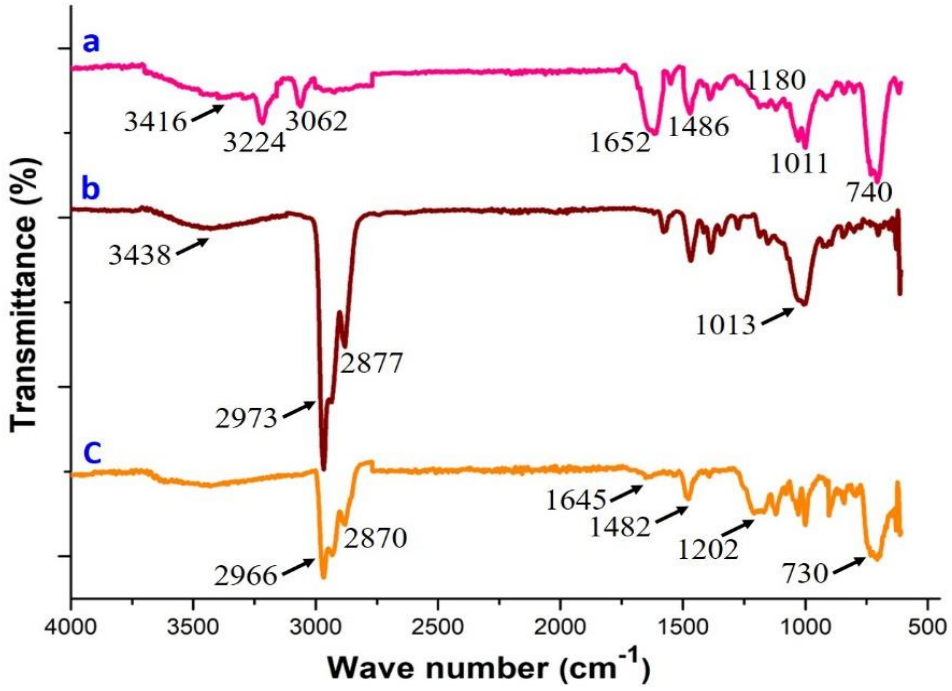

Fig.3. FTIR spectra of a) Anionic direct dye, b) Natural nanoclay and c) Natural nanoclay after adsorbed Anionic direct dye.

FTIR spectral analysis provides crucial information regarding mutual interactions and confirms changes in the functional groups that serve as potential adsorption sites on the natural nanoclay surface. As presented in Fig. 3a, the spectrum for the pure Anionic direct dye has the significant vibrational modes at 3416, 3224, and 3062 cm^{-1}, which correspond to the O-H, N-H, and aromatic C-H functional groups, respectively. The amide O=C-NH group exhibits a low vibrational mode around 1652 cm^{-1}, attributed to the formation of intramolecular hydrogen bonds. Additional modes located at 1540 and 1486 cm^{-1} are assigned to C=C and C=N bonds within the aromatic rings and azo groups (Anirudhan T.S., et.al 2015). The multiband region between 1180–1000 cm^{-1} is ascribed to the C-O and C-N single bonds, while the characteristic out-of-plane bending vibration of aromatic C-H is observed at 740 cm^{-1}. Figure 3b exhibits the main characteristic bands of pristine natural nanoclay at 3438 and 1571 cm^{-1}, corresponding to the hydroxyl group O-H stretch and the H_2O deformation mode, respectively (Bel Hadjltaief H., et.al 2019), (Shashikala B. S., et.al 2026). The band at 1469 cm^{-1} is may be attributed to the trace carbonate (CO_3^{2-}) impurities naturally present within the pristine raw clay sample (Cherian C., et.al 2018), (Shashikala BS, et.al 2022). Furthermore, the spectrum displays characteristic multi-bands associated with the silica (Si-O-Si) framework within the 1180–650 cm^{-1} (El Haouti R., et.al 2018), (Mohammed A. H. Dhaif-Allah, et.al 2025). The FTIR spectrum of the natural nanoclay after adsorbed anionic direct dye (Fig. 3c), displays significant shifts and alterations in vibrational modes compared to the pure anionic direct dye. The clear reduction in intensity, or near disappearance, of the vibrational modes at 3416, 3224, 3062, and 1652 cm^{-1} (associated with the dye's O-H, N-H, and amide functional groups) indicates surface immobilization and adsorption interactions between the natural nanoclay surface and these specific functional groups, rather than a chemical modification of the dye molecule itself. Similar shifts and intensity changes witnessed in the characteristic natural nanoclay bands within the 2973 and 1571–1013 cm^{-1} regions further confirm the surface coverage and adsorption affinity between the natural nanoclay adsorbent and the anionic direct dye.

Optical Behavior

The optical properties of the pure natural nanoclay and the anionic direct dye were analyzed via UV-Vis spectroscopy. For the pristine natural nanoclay (Fig.4a), the optical absorbance spectrum recorded in the wavelength range of 200–800 nm exhibited distinct absorption peaks at 214 and 254 nm, along with a sharp, high-intensity maximum absorption peak at 295 nm. An absorption edge for the material was observed at 326 nm, above which no further peaks were detected, leaving a completely flat baseline across the entire visible light region. This indicates that the pure nanoclay is highly active in the ultraviolet region but remains optically transparent to visible light (Mittal V.et.al, 2010).

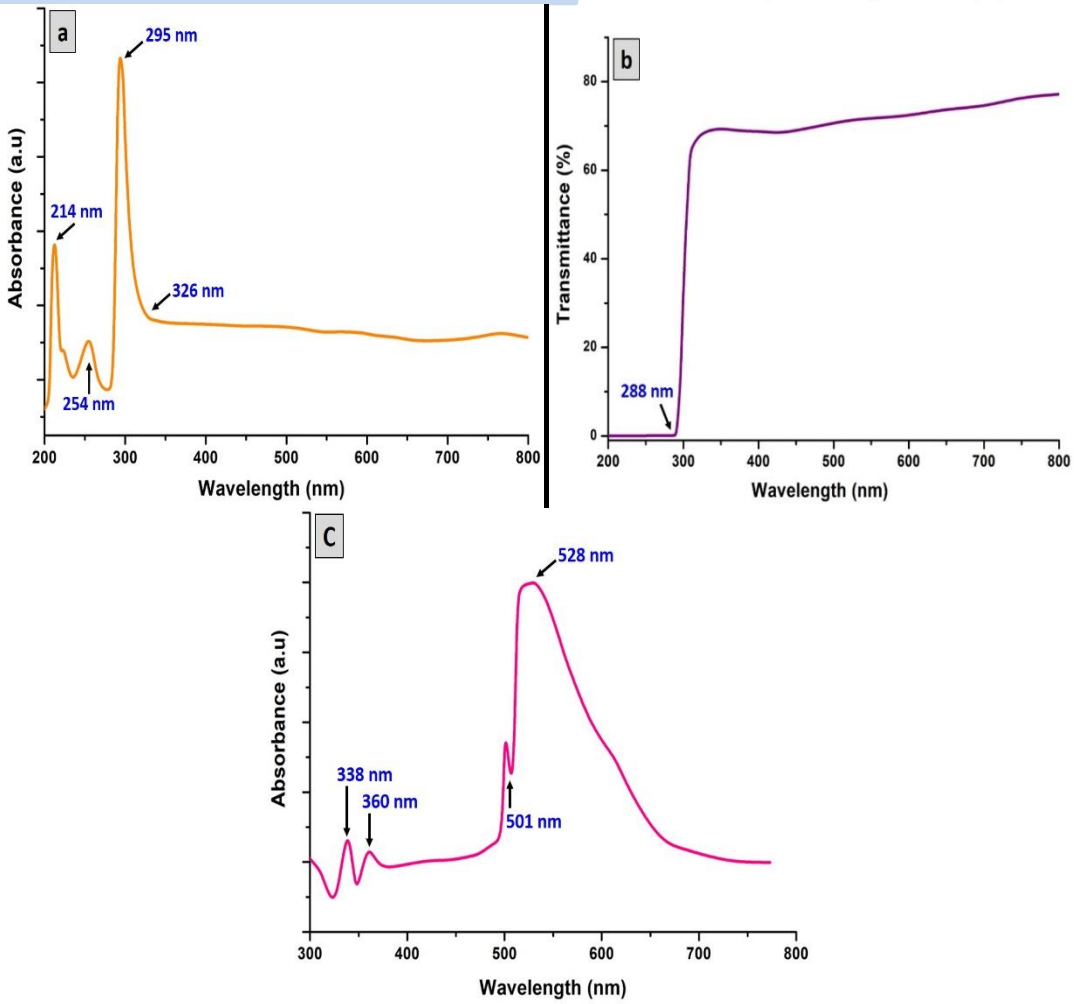

Fig. 4. Optical properties: (a) UV-Vis absorbance and (b) transmittance (%) spectra of pure natural nanoclay; and (c) absorbance spectrum of pure anionic direct dye.

To further evaluate this behavior, the optical transmittance (T%) spectrum of the pure nanoclay was analyzed over the same wavelength range (Fig.4b). The recorded baseline remained completely flat between 200 and 288 nm, confirming that the material does not transmit any light in this deep ultraviolet zone due to electronic transitions between the valence and conduction bands (Pratiwi R. A., et.al 2022). Beyond this threshold, the transmittance sharply arose to reach 77.14%, reinforcing the presence of a pronounced optical band gap edge. For comparative evaluation, the optical absorbance of the pure anionic direct dye was also recorded as presented in Fig.4c. The dye displayed minor peaks in the UV region at 338 and 360 nm, accompanied by a characteristic high-intensity maximum absorption peak at 528 nm and a smaller shoulder peak at 501 nm. This prominent absorption in the visible spectrum at 528 nm confirms the strong colored

nature of the anionic dye, originating from the $\pi \longrightarrow \pi^*$ and $n \longrightarrow \pi^*$ electronic transitions within its conjugated chromophore network (Hassaan M. A., et.al 2017), (Mahmoodi N. M., et.al 2011). This distinct visible peak makes UV-Vis spectroscopy an ideal tool for monitoring its remediation during subsequent batch adsorption experiments.

To further evaluate the electronic structure and active nature of the pure nanoclay, the optical band gap energy (E_g) was determined from the observed spectral edges using the standard fundamental relationship ($E_g = 1240/\lambda_{edge}$), where the λ_{edge} is the absorption edge from Fig.4a. Based on the absorption threshold of 326 nm absorption edge yielded a localized band gap value of 3.8 eV (Pratiwi R. A., et.al 2022). This value indicates that the natural nanoclay behaves as a wide-bandgap insulator or insulator-like semiconductor. This energy state reflects a stable framework that does not easily undergo electronic breakdown under normal visible light exposure, which supports its durability during operations (Mittal V., 2010). From an adsorption standpoint, this wide band gap and the absorption in the UV region indicate a stable surface matrix (Abd El-Latif M. M., et.al 2010). Because electronic band gap limits do not directly dictate dark batch adsorption operations, this optical profile primarily substantiates the structural stability of the material under light exposure. Consequently, the pristine surface area and the native cation exchange capacity remain available for physical and chemical dye binding. This distinct optical profile confirms the material's suitability for the batch adsorption process, allowing for the direct capturing and trapping of the bulky anionic direct dye molecules without light interference or degradation of the adsorbent structure.

Adsorption Behaviors

The time-dependent decolorization of the anionic direct dye by the natural nanoclay was monitored via UV-Vis spectroscopy (Fig. 5a).

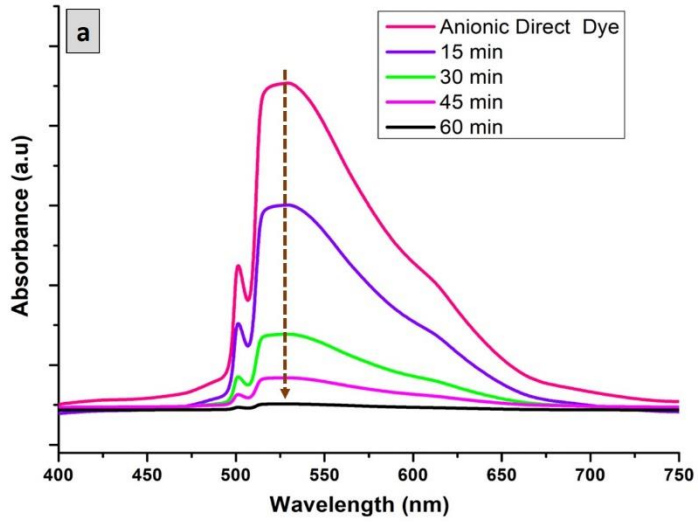

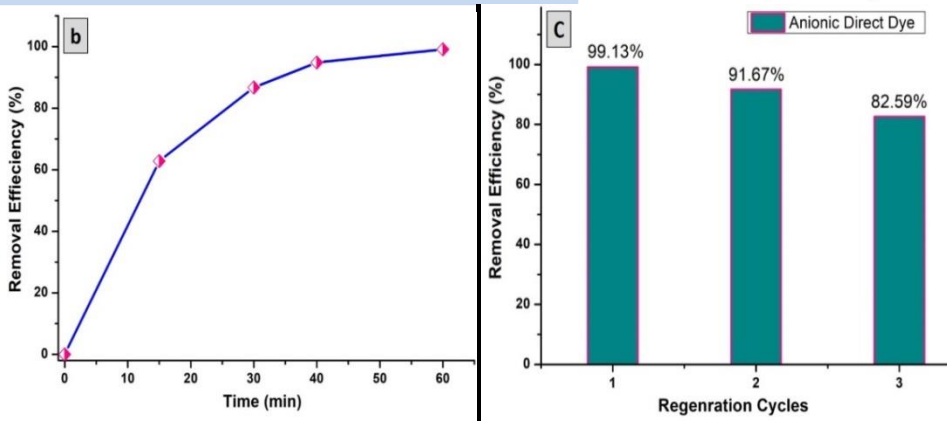

Fig.5. a) Time-dependent absorbance of anionic Direct Dye after treatment with natural nanoclay, (b) Effect of contact time on the removal efficiency of anionic Direct dye, and (c) reusability performance of natural nanoclay over three consecutive cycles.

As shown in Fig. 5a and Table 1, the characteristic absorption peak at λ_{max} = 528 nm exhibited a drastic reduction in intensity as contact time increased from 0 to 60 minutes. Specifically, the absorbance dropped sharply from an initial value of 0.347 to 0.129 within the first 15 minutes, eventually reaching a negligible value of 0.003 after 60 minutes. This rapid decline in absorbance signifies the high affinity of the natural nanoclay for the anionic direct dye molecules. The significant removal achieved in the initial stages (0–15 min) is attributed to the abundance of vacant active sites on the nanoclay surface and its porous architecture, which facilitates rapid external mass transfer (Uddin M. K., 2017). As time progresses, the remaining dye molecules penetrate the internal pores until equilibrium is approached (Awad A. M., et.al 2019). The near-complete disappearance of the 528 nm peak by 60 minutes indicates that the nanoclay effectively sequesters the dye chromophores from the aqueous solution, a phenomenon commonly observed in efficient clay-based adsorption systems (Rida K., et.al 2020). Under the optimized conditions (pH 7.0, 0.05 g dose), the nanoclay demonstrates promising kinetic performance, making it a remarkably efficient adsorbent for anionic pollutants.

Table 1. Adsorption parameters and performance of natural nanoclay for the removal of anionic Direct dye.

Time (min)	Absorbance (528 nm)	q_e (mg/g)	Removal (%)
0	0.347	0.000	0.000
15	0.129	31.41	62.82
30	0.046	43.37	86.74
45	0.018	47.41	94.81
60	0.003	49.57	99.13

Experimental conditions: Initial dye concentration: 50 mg/L; Adsorbent dosage: 0.05 g; Solution volume: 50 ml; pH:7.0; Temperature (25°C).

As presented in Fig. 5b and Table 1, the data shows a rapid increase in adsorption capacity during the first 30 min, where the q_e reached 43.37 mg/g. This high initial rate is attributed to the abundance of vacant active sites on the nanoclay surface. As the process reached 60 min, the q_e stabilized at 49.57 mg/g with a near-complete removal of 99.13 %. This indicates that the natural nanoclay has high affinity for the anionic direct dye, likely due to strong surface interactions or interlayer shielding between the dye molecules and the clay layers (Kumar A., et.al 2020).

The proposed adsorption mechanism of anionic Direct Red dye onto natural nanoclay is predominantly governed by a synergistic combination of hydrogen bonding, $n\longrightarrow\pi$ interactions, and interlayer cation bridging, as frequently reported in the literature (Al-Ali A., et.al 2024), (Kumar A., et.al 2020). Under the optimized neutral conditions (pH 7.0), the nanoclay framework and its edges are predominantly deprotonated and negatively charged, which naturally induces an electrostatic repulsion against the anionic sulfonic groups ($-SO_3^-$) of the dye. However, this repulsion is effectively overcome through cation bridging mediated by the exchangeable divalent interlayer cations (Ca^{2+}. Mg^{2+}) naturally present within the pristine clay matrix (Abd El-Latif M. M., et.al 2010). Furthermore, the large conjugated aromatic system of the Direct Red dye facilitates $n\longrightarrow\pi$ interactions with the oxygen-rich silica sheets, while the amino or azo groups in the dye structure form robust hydrogen bonds with the hydroxyl-terminated surfaces of the nanoclay (Mahdavinia G. R., et.al 2014), (Sadeghi M., et.al 2024). The observed results, which show a sharp increase in removal efficiency during the first 30 min, indicate a two-step process: a rapid initial uptake driven by the high availability of external surface sites, followed by a slower intra-particle diffusion phase where dye molecules penetrate the clay's interlayer galleries (Salam M. A., et.al 2017). As the concentration gradient decreases and surface sites become saturated, the system reaches a dynamic equilibrium. The achievement of 99.13% removal at 60 min confirms that the equilibrium state was successfully established, reflecting the exceptionally high affinity of the natural nanoclay framework for complex anionic chromophores under neutral pH conditions (Zarei S., Sadeghi M., et.al 2018), (Zahoor I., et.al 2024).

The regeneration and reusability of natural nanoclay were evaluated to determine its economic viability for industrial applications (Fig. 5c). In the first cycle, the natural nanoclay achieved a near-complete removal of 99.13%. After recovery and drying, the second and third cycles maintained high removal efficiencies of 91.67% and 82.59%, respectively. This decrease in performance is primarily driven by the physical loss of adsorbent mass during repeated washing and high-speed centrifugation cycles under a constant operational dye solution volume (50 mL). Because the initial solution volume was kept constant across all cycles, this physical mass loss inherently reduced the operational adsorbent dosage ratio, directly decreasing the total number of available active sites for subsequent runs (Zhang L., et.al 2024).

Additionally, partial site blockage caused by the occupation of internal active sites by residual dye molecules that are difficult to fully desorb further contributed to the decline (Tahir M. A., et.al 2024).

Nevertheless, the ability of the natural nanoclay to maintain over 80% efficiency in the third cycle aligns with recent findings on the durability of clay-based nanocomposites (Alsaiari M., et.al 2024). and confirms its promising structural stability. These results validate the natural nanoclay framework as a sustainable, cost-effective, and industrially viable adsorbent for large-scale wastewater treatment (Weng C. H., et.al 2010).

Comparative Performance Analysis

To evaluate the practical efficiency of the natural nanoclay synthesized in this work, its performance was benchmarked against various clay-based adsorbents reported in literature for anionic dye removal (Table 2). The natural nanoclay demonstrated an outstanding removal efficiency of 99.13%, which is significantly higher than results reported for other raw materials, such as smectite-rich natural clay (80.00%) (Rida K., et.al 2020), and raw inorganic clay (~85.00%) (Toor M., et.al 2012). Furthermore, the adsorption capacity (q_e) of 49.57 mg/g observed in this work is highly competitive with other natural montmorillonite variants utilized for Direct Red 23 (47.50 mg/g) (Abd El-Latif M. M., et.al 2010).

Table 2. Comparative adsorption performance of nanoclay-based materials for anionic dyes.

Adsorbent Type	Dyes	q_e (mg/g)	Removal (%)
Natural Montmorillonite clay	Direct Red 23	47.50	90.03% (Abd El-Latif M., et.al 2010)
Na-Montmorillonite clay (Sodic)	Nylosan Red N	170.11	95.00% (El-Mouzdahir Y., et.al 2010)
Untreated Natural Clay	Direct Red 80	—	93.08% (Errais E., et.al 2011)
Natural clay (Smectite-rich)	Acid Brown 75	8.33	80.00% (Rida K., et.al 2020)
Natural red clay	Bright Green	—	96.00% (Nandi B. K., et.al 2009)
Raw inorganic clay	Nylosan Red N	62.05	85.00% (Toor M., et.al 2012)
Na-rich clay composite	Anionic Dye (ADY)	13.39	96.00% (Sahnoun S., et.al 2021)
Natural Halloysite	Anionic Dye (Azurol)	—	99.90% (Kausar A., et.al 2018)
GQD/MMT Nanocomposite*	Congo Red (CR)	—	63.40% (Sharifi K.M., et.al 2024)
Natural Montmorillonite (MMT)	Reactive Red	20.20	83.90% (Raj aei G. E., et.al 2023)
Natural nanoclay (MNC)	Anionic Direct Red	49.57	99.13% (**Present work**)

*GQD/MMT: Graphene Quantum Dot/Montmorillonite nanocomposite

Notably, recent studies on complex systems, such as the GQD/MMT nanocomposite (Sharifi K.M., et.al 2024), and specialized montmorillonite for Reactive Red (Rajaei G. E., et.al 2023), reported removal efficiencies of 83.90% (pH 2.0), and lower capacities (20.20 mg/g), respectively. This indicates that our unmodified natural nanoclay provides superior performance even when compared to modern, chemically

intensive composites. While sodium-saturated (sodic) clays can exhibit higher absolute capacities such as Na-Montmorillonite at 170.11 mg/g (El-Mouzdahir Y., et.al 2010). these materials require rigorous chemical pre-treatments that increase operational costs and complexity. In contrast, the natural nanoclay in this study achieves nearly complete removal of anionic Direct Red under neutral pH conditions without any modification. This high efficiency, coupled with robust reusability and environmental safety, validates the natural nanoclay as a superior, eco-friendly, and cost-effective candidate for the large-scale remediation of textile wastewater (Kausar A., et.al 2018).

Limitations and Future Work

While this investigation confirms that pristine natural nanoclay serves as an efficient, low-cost precursor for the remediation of anionic direct dyes using accessible laboratory facilities, certain experimental boundaries should be acknowledged. This work primarily focuses on validating the macroscopic feasibility, optical properties, and direct reusability of the material without exhaustive sub-microscopic tracking. Additionally, the decline in regeneration efficiency was partially driven by cumulative physical mass loss during consecutive washing cycles under a fixed operating volume, which inherently reduced the net quantity of available active sites. To transition this baseline framework into large-scale applications, several avenues must be explored in future investigations. Advanced structural tracking using X-ray Diffraction (XRD) and Transmission Electron Microscopy (TEM) before and after adsorption is needed to map interlayer spacing variations and spatial dye distribution. Furthermore, a broader operational matrix should systematically evaluate the coupled influences of initial dye concentration, adsorbent dosage, pH, temperature, and full thermodynamic modeling. Finally, future work should investigate surface engineering pathways, such as acid activation or doping with elements like Copper (Cu) or Silver (Ag), while evaluating the bioactivity and antimicrobial performance of these modified matrices to develop multifunctional water purification systems.

Conclusion

This study successfully demonstrates the high-performance capabilities of natural nanoclay (MNC) as a sustainable and cost-effective adsorbent for the remediation of anionic Direct Red dye from aqueous environments. Optical characterization revealed that the natural nanoclay possesses a wide bandgap of 3.8 eV and a strong UV-absorption threshold at 288 nm, providing a stable and electronically active framework for efficient dye capture. Experimental results confirmed that the nanoclay achieves an outstanding removal efficiency of 99.13% within only 60 min under neutral pH conditions, with a maximum adsorption capacity (q_e) of 49.57 mg/g. The adsorption mechanism was identified as a synergistic result of hydrogen bonding, $n \rightarrow \pi$ interactions, and interlayer cation bridging, following a rapid two-step process of surface uptake and intra-particle diffusion. Furthermore, the natural nanoclay exhibited promising regeneration potential, maintaining a high removal efficiency of 91.67% and 82.59% in the second and third cycles, respectively. This performance decline was primarily driven by physical mass loss under a constant operational volume, which

reduced the net quantity of available active sites, alongside residual site blockage. These findings highlight that natural nanoclay is a competitive, scalable, and eco-friendly solution for the treatment of industrial textile wastewater.

References

[1] Zarei S., Sadeghi M., Rezanejade B. G., Dye removal from aqueous solutions using novel nanocomposite hydrogel derived from sodium montmorillonite nanoclay and modified starch. International Journal of Environmental Science and Technology, 15(11) (2018) 2303–2316.

[2] Murad Q.A. Al-Gunaid, Gayitri H. M., Shashikala B.S, Waleed Abdo, Mohammed A.H. Dhaif-Allah, Fares H. AL-Ostoot. Metal oxide nanofillers induced changes in material properties and related applications of polymer composites. European Journal of Chemistry, 14(2023)1-14.

[3] Alkanad Khaled, Hezam Abdo, Sujay Shekar, Drmosh, Q. A, Amrutha K, Murad. Q. A.AL-Gunaid, Lokanath, N. K, Magnetic recyclable α-Fe_2O_3-Fe_3O_4/Co_3O_4-CoO nanocomposite with dual Z-scheme charge transfer pathway for quick photo-Fenton degradation of organic pollutants. Catalysis Science & Technology, 11 (2021) 3084-3097.

[4] Anupama, B. H, Murad Q.A. Al-Gunaid, Siddaramaiah, Performance of nano K-doped zirconate on modified opto-electrical and electrochemical properties of gelatin biopolymer nanocomposites. Polymer Bulletin, 78 (2021) 3023–3041.

[5] Gayitri H M, Murad Q. A. AL-Gunaid, Siddaramaiah and Gnana Prakash A. P., Investigation of triplex $CaAl_2ZnO_5$ nanocrystals on electrical permittivity, optical and structural characteristics of PVA nanocomposite films. Polymer Bulletin, 77 (2020) 5005–5026.

[6] Mahdavinia G. R., Massoudi, A., Baghban A., Massoudi R., Synthesis of Na-montmorillonite nanocomposites for crystal violet adsorption. Journal of Applied Polymer Science, 131(4) (2014)39912.

[7] Murad Q. A. AL-Gunaid, Waleed Abdo, Mohammed A.H. Dhaif-Allah, Fares H. AL-Ostoot., Photo-Electrical Tandem of Modulated Polyvinyl Alcohol Based Plasticized Solid Polymer Electrolyte Nanocomposite Films: Effect of Propylene Carbonate Contents. TUJNAS, 8(1) (2023) 39 – 55.

[8] Gayitri H.M., Murad Q. A. AL-Gunaid, Kumar, J.R., Investigation on optical, structural and electrochemical properties of hybrid PVA/$ZnWMoO_7$ nanocomposite film for optoelectronics and super capacitor applications. Polymer Bulletin, 80 (2023) 8665-8683.

[9] Somesh T. E, Murad Q.A. Al-Gunaid, Madhukar B.S and Siddaramaiah: Photosensitization of optical band gap modified PVA films with hybrid $AgAlO_2$ nanoparticles. J. Mater. Sci.: Materials in Electronics, 30 (2018) 37-49.

[10] Kumar R., Kumar M., Upadhyay S. N., Efficacy of nanoclays as the potential adsorbent for dyes and wastewater systems. Environmental Technology & Innovation, 20 (2020)101132.

[11] Mohammed A. H. Dhaif Allah and Akheel Ahmed Syed., Development of Sustainable Dye Adsorption System Using Nutraceutical Industrial Turmeric Root Spent-Studies with Direct Red 13. Int J Recent Sci Res. 9(2) (2018) 24370-24380.

[12] Murad Q. A. Al-Gunaid, Waleed A. Abdulrab, Mohammed A. H. Dhaif-Allah, Ahmed Qaid, Waleed Al-Ghabri, Fares H. Al-Ostoot, Preparation of nano-graphene oxide and its reduction via a natural extract for its application as a photocatalyst in purifying water contaminated by malachite green dye. Sci J Fac Educ., 14(1) (2025)9–29.

[13] Almasri D. A., Saleh N. B., Atieh M. A., McKay G., Ahzi S., Hydroxy iron modified montmorillonite (HyFe-MMT) nanoclay for arsenic removal. Chemical Engineering Journal, 345(2018)126–134.

[14] Mohammed A. H. Dhaif Allah and Akheel Ahmed Syed. 2018, Use of Kaolinite as an Adsorbent: Equilibrium and Dynamics of Adsorption of Direct red 13 from Aqueous Solution. Int J Recent Sci Res. 9(8), pp. 28260-28269.

[15] Zaharia C., Suteu D., Textile organic dyes: Characteristics, polluting effects and separation/elimination procedures from industrial effluents A critical overview. In Organic Pollutants, 3 (2012)55–86.

[16] Mittal A., Gupta V. K., Malviya A., Mittal J. Adsorptive removal of dyes from wastewater. Journal of Environmental Management, 90(8) (2009) 2413–2424.

[17] Sonawane S. H., Chaudhari P. K., Ghodke S. A., Parande A. K., Patil S. V., Ultrasound-assisted synthesis of poly (acrylic acid)-nanoclay composites for dye removal. Ultrasonics Sonochemistry, 16(1) (2009) 48–55.

[18] Mahvi A. H., Ghanbari F., Moradi M., Dalvand A., Adsorption of Direct Red 23 dye from aqueous solution by means of modified montmorillonite nanoclay as a superadsorbent: Mechanism, kinetic and isotherm studies. Journal of the Taiwan Institute of Chemical Engineers, 116 (2020) 178–188.

[19] Mouton J., Mbhele Z., Katata-Seru, L., The promising applications of nanoparticles for synthetic dyes removal. Management of Environmental Quality, 33(2) (2022) 451–470.

[20] Zahoor I., Javeed A., Nazir R., Bashir A., Tailored nanoclay blends for enhanced dye mixture removal from aqueous environments. Elsevier Materials Today Communications, 38 (2024) 108341.

[21] Shashikala B.S, Murad Q.A. Al-Gunaid, T. E. Somesh, Anasuya S.J & Siddaramaiah, Core–shell synergistic effect of (PANI-$NaBiO_2$) incorporated polycarbonate films to photodegradation of MG dye and photovoltaic activity. Polymer Bulletin, 79 (2021) 7531-7554.

[22] Al-Ali A., Al-Amrani M., Investigating dye adsorption: The role of surface-modified montmorillonite nanoclay in kinetics, isotherms, and thermodynamics. Zeitschrift für Physikalische Chemie, 238(5) (2024) 785–802.

[23] Mittal V., Characterization Techniques for Polymer Nanocomposites. Wiley-VCH Verlag GmbH & Co., (2010)1–25.

[24] Abd El-Latif M. M., Ibrahim A. M., El-Kady M. F., Adsorption of dyes using different types of clay: a review. Applied Water Science, 1 (2010) 1–15.

[25] Salam M. A., Kosa S. A., Al-Beladi A. A., Application of nanoclay for the adsorptive removal of Orange G dye from aqueous solution. Journal of Molecular Liquids, 241 (2017) 469–477.

[26] Sadeghi M., Hosseinzadeh H., Mahmoodi N. M., Studying removal of anionic dye by prepared highly adsorbent nanocomposite hydrogel. Scientific Reports, 14 (2024) 5214.

[27] Hassaan M. A., El Nemr A., Health and environmental impacts of dyes: Mini review. American Journal of Environmental Science and Engineering, 1(3) (2017) 64–67.

[28] Mohammed A. H. Dhaif Allah, Taqui S. N., Syed U. T., Akheel A. Syed, Ukkund S. J., Khan W.A., Water footprint management in textile industry through Acid Blue 113 remediation using halloysite nanoclay as a sustainable adsorbent. Scientific Reports, 15 (2025) 13698.

[29] Ait Akbour R., Ouachtak H., Jada A., Akhouairi S., Ait Addi A., Douch J., Hamdani M., Humic acid covered alumina as adsorbent for the removal of organic dye from coloured effluents. Desalin. Water Treat., 112 (2018) 207–2017.

[30] Farhad M., Mohsen J., Adsorption of ammonium from simulated wastewater by montmorillonite nanoclay and natural vermiculite: experimental study and simulation. Environ Monit Assess, 189 (2017) 415 (1-19).

[31] Ukkund S.J., Puthiyillam P., Alshehri H.M., Goodarzi M., Taqui S.N., Anqi A.E., Safaei M.R., Ali M.A., Syed U.T., Mir R.A., Adsorption Method for the Remediation of Brilliant Green Dye Using Halloysite Nanotube: Isotherm, Kinetic and Modeling Studies. Appl. Sci. 11(2021) 8088.

[32] Murray H. H., Overview-clay mineral applications. Applied Clay Science,5 (1991) 379–395.

[33] Anirudhan T.S., Ramachandran M., Adsorptive removal of basic dyes from aqueous solutions by surfactant modified bentonite clay (organoclay): kinetic and competitive adsorption isotherm. Process Saf. Environ. Prot. 95 (2015) 215–225.

[34] Bel Hadjltaief H., Galvez M.E., Ben Zina M., Da Costa P., TiO_2/clay as a heterogeneous catalyst in photocatalytic/photochemical oxidation of anionic reactive blue 19. Arab. J. Chem. 12(2019) 1454–1462.

[35] Shashikala B. S., Murad Q. A. AL-Gunaid, Gayitri H.M., Mohammed A. H. Dhaif-Allah, Waleed A. Abdulrab, Sultan A. Al-horaibi, Fares H. Al-Ostoot, Synergistic impact of core-shell PANI/HNT nanofillers in polycarbonate films: engineering structural integrity, electrical permittivity, and thermal stability for advanced energy storage systems. Inorganic Chemistry Communications, 184 (2026) 115990 (1-15).

[36] Cherian C., Kollannur N.J., Bandipally S., Arnepalli D.N., Calcium adsorption on clays: effects of mineralogy, pore fluid chemistry and temperature. Appl. Clay Sci.160 (2018) 282–289.

[37] Shashikala BS, Murad QA, AL-Gunaid FH, Al-Ostoot N, Al-Zaqri A, Boshaala, Siddaramaiah, Anasuya SJ., Probing optical efficiency and electrochemical behaviors of polycarbonate incorporating conducting PANI and Halloysite nanotubes (HNTs) as core–shell nanofillers. Polym Bull., 79 (2022)10333–55.

[38] El Haouti R., Anfar Z., Et-Taleb S., Benafqir M, Lhanaf S., El Alem N., Removal of heavy metals and organic pollutants by a sand rich in iron oxide, Euro-Mediterr. J. Environ. Integr. (2018) 3–17.

[39] Mohammed A. H. Dhaif-Allah, Ahmed Qaid, Murad Q. A. AL-Gunaid, Waleed A. Abdulrab, Morad G. Al-asbahi, Waleed Al-Ghabri, B. S. Shashikala, Sultan A. Al-horaibi, Fares H. Al-Ostoot, Ecofriendly synthesis and antibacterial assessment of silver and copper nanoparticles using Solanum incanum L. extracts, Discover Chemistry, 2 (2025) 293 (1-23).

[40] Pratiwi R. A., Nandiyanto, A. B. D., How to read and interpret UV-VIS spectrophotometric results in determining the structure of chemical compounds. Indonesian Journal of Educational Research and Technology, 2(1) (2022) 1–20

[41] Mahmoodi N. M., Salehi R., Arami M., Bahrami H., Dye removal from colored textile wastewater using chitosan in binary systems. Desalination, 267(1) (2011) 64–72.

[42] Uddin M. K., A review on the adsorption of heavy metals by clay minerals, with special focus on the past decade. Chemical Engineering Journal, 308 (2017) 438–462.

[43] Awad A. M., et al., Adsorption of organic pollutants by natural and modified clays: A comprehensive review. Separation and Purification Technology, 228 (2019) 115719.

[44] Rida K., et al., Adsorption of anionic dye on natural and modified clays: Surface and thermodynamic studies. Journal of Saudi Chemical Society, 17(3) (2013)239–245.

[45] Kumar A., et al., Enhanced adsorption of anionic dyes on natural clay: Mechanism and kinetic studies. Environmental Nanotechnology, Monitoring & Management, 14 (2020) 100341.

[46] Zhang L., et al., Advances in magnetic nanocomposite adsorbents for water treatment: Recovery and secondary pollution challenges. Molecules, 29(18) (2024) 4381.

[47] Tahir M. A., et al., Studying removal of anionic dye by prepared highly adsorbent nanocomposite: Regeneration and reusability studies. Scientific Reports, 14 (2024) 9115.

[48] Alsaiari M., et al., Synthesis, characterization, and application of novel reusable natural clay nanocomposites for dye removal. Adsorption Science & Technology, 42 (2024) 1279038.

[49] Weng C. H., et al., Enhancing removal efficiency of anionic dye by combination and calcination of natural clays. Journal of Hazardous Materials, 171 (2009) 481-489.

[50] Abd El-Latif M. M., et al., Kinetic and equilibrium studies of direct dye adsorption on clay, Desalination, 259(1-3) (2010) 230–239.

[51] El-Mouzdahir Y., et al., Adsorption of methylene blue and nylosan red from aqueous solutions onto clay, Powder Technology, 201(1) (2010) 64–74.

[52] Errais E., et al., Efficient adsorption of anionic dye from aqueous solutions on untreated natural clays. Applied Clay Science, 54(3-4) (2011) 273–281.

[53] Nandi B. K., et al., Adsorption of Brilliant Green dye from aqueous solution onto kaolinite and montmorillonite: A comparative study, Journal of Hazardous Materials, 164(2-3) (2009) 646–660.

[54] Toor M., Jin B., Adsorption characteristics, isotherms and kinetic studies of anionic dyes onto natural bentonite or mixed iron oxides. Chemical Engineering Journal, 184 (2012) 118–130.

[55] Sahnoun S., Boutahala M., Cationic and anionic dye adsorption on a natural clayey composite: Drimaren Yellow (ADY) removal. Applied Sciences, 11(11) (2021) 5127.

[56] Kausar A., et al., Adsorption of anionic dyes from aqueous solution using natural and modified halloysite nanotubes: A review. Journal of Molecular Liquids, 256 (2018) 395–407.

[57] Sharifi K.M., Marjani A.P., Balkanloo P.G., Enhanced dye removal using montmorillonite modified with graphene quantum dots in sustainable salep nanocomposite hydrogel. Scientific Reports, 14 (2024) 12432.

[58] Rajaei G. E., et al., Removal of Reactive Red-P2B from aqueous solutions by montmorillonite clay; Kinetics, thermodynamic and isotherm studies. Inorganic Chemistry Communications, 149 (2023) 110386.

❊❊❊